Anisotropy of Chemical Bonding in Semifluorinated Graphite C_2F Revealed with Angle-Resolved X-ray Absorption Spectroscopy

Alexander V. Okotrub,[†,*] Nikolay F. Yudanov,[†] Igor P. Asanov,[†] Denis V. Vyalikh,[‡] and Lyubov G. Bulusheva[†]

[†]Nikolaev Institute of Inorganic Chemistry, SB RAS, 3 Academician Lavrentiev ave., 630090 Novosibirsk, Russia and [‡]Institute of Solid State Physics, Dresden University of Technology, 01062 Dresden, Germany

ABSTRACT Highly oriented pyrolytic graphite characterized by a low misorientation of crystallites is fluorinated using a gaseous mixture of BrF_3 with Br_2 at room temperature. The golden-colored product, easily delaminating into micrometer-size transparent flakes, is an intercalation compound where Br_2 molecules are hosted between fluorinated graphene layers of approximate C_2F composition. To unravel the chemical bonding in semifluorinated graphite, we apply angle-resolved near-edge X-ray absorption fine structure (NEXAFS) spectroscopy and quantum-chemical modeling. The strong angular dependence of the CK and FK edge NEXAFS spectra on the incident radiation indicates that room-temperature-produced graphite fluoride is a highly anisotropic material, where half of the carbon atoms are covalently bonded with fluorine, while the rest of the carbon atoms preserve π electrons. Comparison of the experimental CK edge spectrum with theoretical spectra plotted for C_2F models reveals that fluorine atoms are more likely to form chains. This conclusion agrees with the atomic force microscopy observation of a chain-like pattern on the surface of graphite fluoride layers.

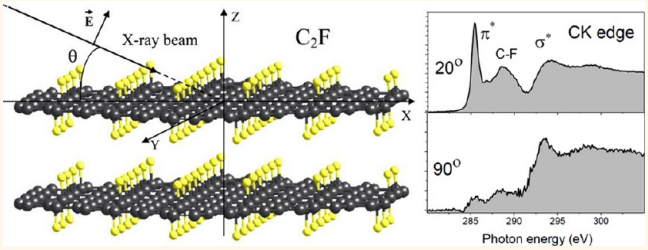

KEYWORDS: layered materials · fluorination · graphene · X-ray absorption · DFT calculation

Since the successful attempt of micromechanical detachment of one-atom-thick layers from graphite crystal,[1] the layered compounds attract a lot of attention as precursors of 2D materials.[2] The appearance of other properties in 2D crystals as compared with their 3D counterparts encourages scientists to look for new candidates for exfoliation as well as to modify chemically the obtained layers. Graphene was shown to covalently attach oxygen,[3] hydrogen,[4,5] and fluorine,[6,7] which opens an energy gap of initially zero.[8] In graphene oxide, the various oxygen-containing groups are randomly distributed over the sheet, while each carbon atom may be singly bonded with a hydrogen or fluorine atom, yielding stoichiometric derivatives of graphene−graphane $(CH)_n$ and fluorographene $(CF)_n$. Varying the loading of foreign atoms, one can tune the band gap in hydrogenated and fluorinated graphene.[9,10] This property is very important for the development of 2D materials with desirable optical and transport characteristics.[11]

Similar to graphite crystal, graphite fluorides are characterized by strong covalent in-plane bonding and weak van der Waals-like coupling between the layers that make it possible to obtain fluorinated graphene layers that exfoliate the bulk materials mechanically[12] or in organic solution.[13] Two stoichiometric forms, poly(carbon monofluoride) $(CF)_n$ and poly(dicarbon monofluoride) $(C_2F)_n$, are known presently.[14] X-ray powder diffraction study of microcrystals of $(CF)_n$ indicated that fluorine atoms are subsequently bonded with both sides of the graphene sheet producing a chair conformation of carbon hexagons.[15] Density functional theory (DFT) calculation showed that the 3D $(CF)_n$ crystal should be a semiconductor with a direct band gap of 3.5 eV.[16] Calculations of fluorographenes confirmed

* Address correspondence to spectrum@niic.nsc.ru.

Received for review May 2, 2012 and accepted December 7, 2012.

Published online December 07, 2012
10.1021/nn305268b

that the chair conformation is the most stable energetically, and layer stacking should have no considerable effect on the electronic and optical properties of the 3D structure.[17,18] The reason is a large interlayer spacing in $(CF)_n$ equal to ~0.59 nm.[19] While direct fluorination of graphite to the CF composition requires high temperatures (from 600 to 640 °C),[20] semifluorinated graphite $(C_2F)_n$ is prepared at milder conditions. The structure of this compound is unknown, and it is suggested that $(C_2F)_n$ synthesized at elevated temperatures of 350−400 °C using elemental fluorine actually consists of fluorinated bilayers with interior covalent bonds between bare carbon atoms from the adjacent layers.[21] Since all carbon atoms are in the sp^3 hybridization, the high-temperature-produced $(C_2F)_n$ should be an insulator similar to diamond.

Adding the anhydrous HF to F_2 or use of volatile inorganic fluoride, for example, BrF_3 and ClF_3, as a fluorinating agent allows one to produce graphite fluoride with approximate composition of C_2F at room temperature.[22−24] A part of the molecules is trapped between fluorinated carbon layers, yielding an intercalated graphite fluoride compound.[25] Semiempirical quantum−chemical modeling of the X-ray fluorescent C Kα spectrum of low-temperature semifluorinated graphite synthesized using BrF_3 indicated that the most preferable fluorine pattern is "up" and "down" (1,2)-fluorine addition with formation of CF chains alternating with bare carbon chains.[26] Existence of π electrons in C_2F layers is likely responsible for magnetic ordering in the intercalated semifluorinated graphite compounds detected at low temperatures.[27] Alternatively, $(C_2F)_n$ can be considered as a mixture of graphene and fluorographene $(CF)_n$ layers and, if so, the compound should possess metallic conductivity.[28,29]

Near-edge X-ray absorption fine structure (NEXAFS) spectroscopy is a powerful tool for the examination of the anisotropy of chemical bonding in a compound.[30] In this case, X-ray transitions involve the excitation of electrons from a core level to partially filled or empty states. Due to high localization of core electrons and the dipole selection rules, the spectrum probes the partial density of unoccupied states of an element, which allows identifying the local chemical bonding in the material. The bond orientation is detected from changes in the intensity of corresponding resonances with the incident-polarized X-ray radiation. Thus, measuring the NEXAFS spectra near the CK and FK edge of graphite fluorides $(CF)_n$ and $(C_2F)_n$ synthesized at high temperatures, Seki *et al.* observed the angular dependence of the peaks corresponding to σ^*(CF) excitations.[31] This dependence was ascribed to near vertical orientation of C−F bonds relative to the carbon skeleton. However, the much stronger changes in the spectra are characteristic for anisotropic materials possessing a π system, such as graphite,[32] hexagonal BN,[33] aligned carbon nanotubes,[34] graphene,[35] and graphene oxide films.[36,37]

Here, we use angle-resolved NEXAFS spectroscopy to reveal the chemical bonding in graphite fluoride $(C_2F)_n$ synthesized at room temperature using a gaseous mixture of BrF_3 and Br_2. In planning this work, we have specifically taken the highly oriented pyrolytic graphite (HOPG) to obtain fluorinated flakes of suitable size for the measurements. The fluorine distribution in layers was guessed by comparing the experimental CK edge spectrum with theoretical profiles calculated for three fluorinated graphene models. The excitonic nature of the π^* and σ^* resonances[38] was accounted within the framework of so-called $Z+1$ approximation, where a fictitious $Z+1$ compound with an additional proton in its atomic nucleus is introduced instead of the real Z compound containing a core level hole.[39] In the case of a carbon structure, one carbon atom should be replaced by one nitrogen atom, while an increase in the total number of electrons is compensated by introduction of an additional positive charge. Efficiency of the $Z+1$ approximation has been previously demonstrated for fullerenes C_{60} and C_{70},[40] fluorinated and chlorinated fullerenes $C_{60}F_{36}$[41] and $C_{60}Cl_{30}$,[42] graphene,[43] and carbon nanotubes.[44]

RESULTS AND DISCUSSION

Structural and Composition Characterization. Fluorination of graphite using the saturated vapors of a fluorinating agent requires diffusion of molecules between the layers. At room temperature, this process is a quite slow, and it is why at least 1 month is needed to obtain a sample with C_2F composition. Starting from the edges, the fluorinated area grows toward the central part of a graphite plate. Since the attachment of fluorine atoms to the basal graphene sheets increases the interlayer spacing, the plate is gradually expanded from a periphery. The structure imperfections (stacking faults and dislocations) and large lateral size of the used HOPG sample are likely to cause considerable tension between the outer fluorinated surface region and the inner nonfluorinated core region. As a result, the plate is split into flakes with a characteristic thickness of a few micrometers (Figure 1a). Probably the structural defects that exist in the initial sample hold the flakes together. Identical golden color of the flakes in a stack evidence the fluorination across the whole depth of the sample. Owing to the large space between the flakes, they are easily separated using a knife. Optical microscopy examination shows that detached flakes have multilayered structure and uniform coloring (Figure 1b). Transparence of the outer and interior layers indicates the absence of nonfluorinated graphenes within a flake.

An X-ray diffractogram obtained for the fluorinated HOPG sample kept under the Br_2 vapors revealed the

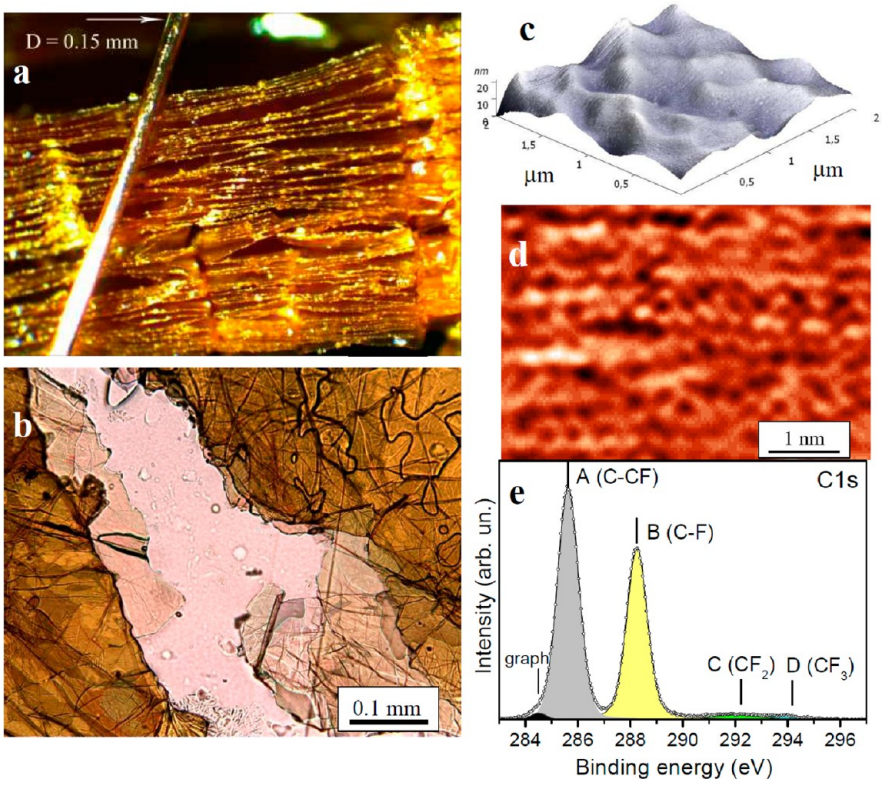

Figure 1. Side view of the fluorinated HOPG plate consistng of golden-colored flakes (a) and transmission optical image of multilayered flake (b). Tapping mode AFM topographic three-dimensional image (c) and filtrated image of the surface (d) of fluorinated HOPG. XPS C 1s spectrum of the fluorinated HOPG with components corresponding to graphite, bare carbon atoms linked with CF groups (C−CF), carbon atoms from CF groups (C−F), and CF_2, CF_3 edge groups (e).

formation of a first-stage intercalation compound with an interlayer distance of ~0.92 nm (Supporting Information, Figure S1). In this compound, Br_2 molecules are accommodated between each fluorinated graphene layer. Drying the sample in nitrogen flow removes the mobile intercalant molecules, yielding a mixed-stage compound with an average distance between adjacent intercalated layers of ~0.78 nm. By weighing, the approximate composition of the product is $C_2F(Br_2)_{0.13}$. The broadening of (00*l*) reflections as compared to those of the initial HOPG could be ascribed to the increase of disordering along the *c*-direction with the graphitic layer fluorination. Actually, the AFM topographic study shows that the fluorinated layers are highly rippled with a correlation length of ~500 nm and a height of ~20 nm (Figure 1c). The image obtained with a high resolution demonstrates structural disordering of the layer surface (Figure 1d). The light regions can be attributed to fluorine atoms rising above the graphitic surface. The atoms are essentially arranged in parallel chains with a length varying from ~0.3 to 3 nm. Sometimes the neighboring chains are linked by CF groups forming the hexagon-like dark regions on the AFM image. Preservation of aromatic carbon hexagons and polyene-like chains in the fluorinated graphite is supported by the appearance in the Raman spectrum of a G mode at 1580 cm^{-1} and scattering within 1400−1520 cm^{-1} respectively (Supporting Information, Figure S2).

The chemical state of carbon in the produced graphite fluoride was evaluated from the XPS C 1s spectrum (Figure 1e). A low-energy component around 284.5 eV corresponds to the sp^2 carbon atom[45] constituted graphitic regions, which were likely to be inaccessible for the fluorinating agent. A small intensity of the component indicates a high structural quality of the HOPG crystal used for the fluorination. Increase of the binding energy of the main C 1s spectral components relative to the graphitic one is due to the change in electronic state of carbon atoms involved in the fluorination process. Intense peak A located at 285.6 eV corresponds to the bare carbon atoms located near the CF groups. The carbon atoms directly bonded with fluorine atoms contribute to the spectral peak B at 288.3 eV. A ratio of intensities of peaks A and B gives a $C_2F_{0.87}$ stoichiometry for the fluorinated regions. The fluorine content estimated from the XPS data is lower than that obtained from the sample weighting, and one of the reasons for this result is the reduction of the fluorinated graphite surface under the action of water vapor present in the surrounding atmosphere.[46] The large size of crystallites in the initial HOPG is supported by the negligible intensity of the components C and D around 292 and 293.9 eV, which are ascribed to the CF_2

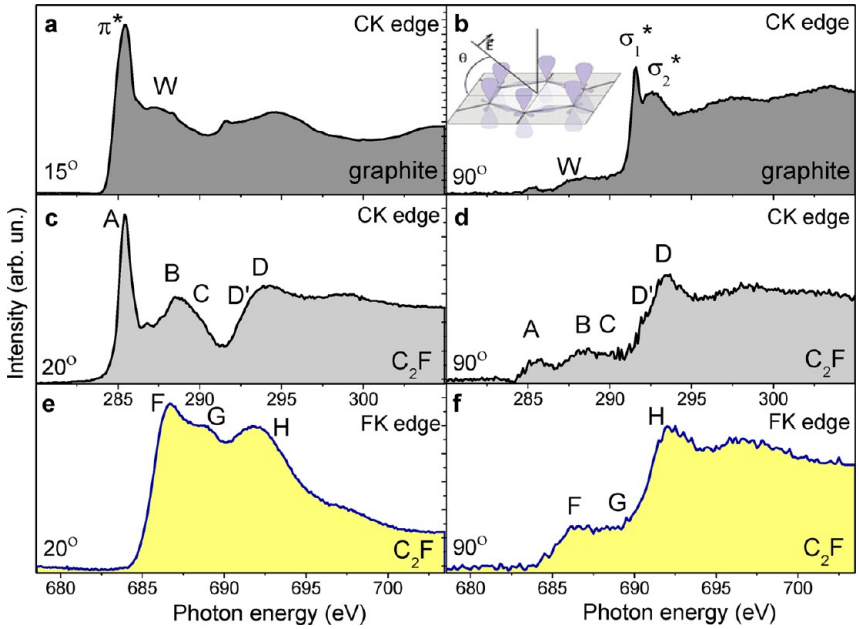

Figure 2. NEXAFS spectra measured near the CK edge of HOPG at an incidence angle θ of radiation of 15° (a) and 90° (b). The inset shows orientation of the electric field vector of synchrotron radiation relative to the basal plane of graphite. NEXAFS spectra of the fluorinated HOPG measured near the CK edge at grazing (c) and normal (d) incidence and near FK edge at grazing (e) and normal (f) incidence.

and CF_3 groups. These groups are developed at the graphene edges.

The XPS F 1s spectrum of the sample has a single peak with a binding energy of ~687.2 eV (Supporting Information, Figure S3a), indicating that all fluorine atoms are covalently attached to the graphitic layers.[47] The previous XPS examination of a set of intercalated compounds of semifluorinated graphite has shown that the position of the F 1s line is independent of the host molecule[48] that could prove an absence of chemical bonding between the intercalant and matrix. The XPS Br 3d spectrum (Supporting Information, Figure S3b) shows that the intercalant molecules are mainly Br_2 with a negligible admixture of BrF_3. Note that binding energy of Br_2 molecules intercalated between the layers of semifluorinated graphite is markedly higher than that detected for the charge transfer carbon black−Br_2 complexes,[49] and this fact supports the conclusion about weak interactions in the Br_2−C_2F system.

Angular Dependence of the NEXAFS Spectra Measured for HOPG and C_2F. First, we demonstrate the potential of angle-resolved NEXAFS on the example of HOPG. The CK edge spectra recorded at close grazing and normal incidence of radiation are compared in Figure 2a,b. The spectra were normalized on the intensity at 330 eV (not shown in the figure). At the grazing angle $\theta = 15°$, the electric field vector of synchrotron radiation is near normal to the sample surface. In this geometry, electron transitions from the C 1s level to unoccupied states of π symmetry have the largest probability that results in the high intensity of π^* resonance appearing at 285.4 eV (Figure 2a). At the normal incident beam, the electric vector lies in the basal plane of graphite, and the dipole selection rules allow the 1s→σ^* transitions only.[50] NEXAFS spectrum measured at $\theta = 90°$ is dominated by a sharp peak located at 291.6 eV and a less intense peak around 292.5 eV (Figure 2b). The peaks are attributed to the σ_1^* and σ_2^* resonances,[51,38] which became well-separated when the spectrum was recorded with very high energy resolution.[52] The negligible intensity of the π^* resonance in the spectrum is indicative of the high crystallinity of HOPG.[53] The origin of a broad feature W around 288 eV is a topic for discussion, and it can be ascribed to the interlayer states of graphite[54,55] and/or graphite functionalization[56] and defects.[43] The intensity and shape of this feature are not changed with the radiation incidence, specifying its isotropic character.

The CK edge NEXAFS spectra of the fluorinated HOPG recorded at incidence angles of 20 and 90° are compared in Figure 2c,d. At the near grazing angle, the spectrum has an intense peak A coinciding with the graphite π^* resonance in energy position (Figure 2c). This fact unambiguously indicates preservation of the π system in the graphite fluoride $(C_2F)_n$ synthesized at room temperature. In contrast to our results, the CK edge spectrum of high-temperature-produced $(C_2F)_n$ showed a very small intensity around 285 eV, confirming that almost all carbon atoms composing the layers are in the sp^3-hybridized state.[31] The peak B at 288.5 eV with a shoulder C around 290 eV should be related to the 1s→σ^* transitions within carbon atoms bonded with fluorine. Actually, the peaks around 288.7 and

290 eV have been observed in the NEXAFS spectra measured near the CK edge of fluorinated activated carbon fibers[57] and fluorinated carbon nanotubes.[58] For the normal incidence, all three mentioned peaks are strongly suppressed in the intensity (Figure 2d), and this fact confirms that peaks A, B, and C are mainly contributed by carbon electrons from orbitals perpendicular to the basal plane. The higher relative intensity of the peak A in the spectrum of $(C_2F)_n$ compared to the intensity at 285.4 eV in the spectrum of pristine graphite (Figure 2b) is caused by the deformation of a graphitic network induced by fluorination as it is observed from the AFM examination of the sample (Figure 1c). The peaks D′ and D are the most prominent in the CK edge spectrum of graphite fluoride recorded at the normal incident X-ray beam. Because intensity of these peaks is independent of the beam direction, they should be assigned to the σ^* states. The transitions to the states of carbon atoms, which are nonbonded and bonded with fluorine atoms, are likely responsible for the resonances at 292 and 293.4 eV, respectively.

To directly determine the orbitals formed with both fluorine and carbon contributions, the CK and FK edge spectra were aligned using a spacing value of 398.5 eV obtained as an energy difference in the F 1s level and the middle position between two main components of the C 1s spectrum. The peak H at 691.8 eV in the FK edge spectrum coincides with the carbon σ^* states (D peak), and hence it should be attributed to the absorption K edge of fluorine (Figure 2e,f). Two pre-edge peaks F and G located at 686.7 and 688.8 eV are overlapped with the peaks B and C in the CK edge spectrum. Recent NEXAFS examination of the fluorinated double-walled carbon nanotubes found a large difference in the fluorine pre-edge structure of the samples produced by different fluorination techniques.[59] Probably, the fluorine peaks F and G and, respectively, the carbon peaks B and C correspond to different local surrounding of CF groups. The strong dependence of the intensity of peaks F and G on the incidence of X-ray radiation shows that the C−F bonds have predominantly perpendicular orientation to the basal plane.

Quantum-Chemical Modeling. A few models of fluorinated graphite and graphene with a C_2F stoichiometry have been considered to date.[26,28,29,60,61] Use of molecular F_2 as a fluorinating agent was predicted to result in formation of double-layered structures where all carbon atoms are in the sp^3-hybridized state (half of the atoms are covalently linked with fluorine, and the other half interacts with carbon atoms from the neighboring layer).[29] In contrast, the fluorination by fluorine atoms should cause alternation of fully fluorinated graphene sheets with the noncovered graphenes. For semifluorinated graphite $(C_2F)_n$ obtained at room temperature, we discard the double-layer models because the NEXAFS CK edge spectrum shows the existence of the sp^2-hybridized carbon atoms in the material and the model preserving intact graphene layers because the XPS C 1s spectrum detects only a negligible portion of this species in the sample. The C_2F models with one side of graphene fluorination[60] are also unsuitable in our case as fluorine access is possible to both sides of the graphite layer. Modeling of HF-catalyzed F_2 addition to graphene revealed that (1,2) and (1,4) addition products have about the same energy[61] that could result in a mixture of different fluorine patterns. For the stoichiometry close to C_2F, these preferable fluorine additions should produce at least three configurations where the chains (armchair or zigzag) constituted from bare carbon atoms alternate with chains from fluorinated carbon atoms and the double C═C bonds alternate with CF−CF bonds (Figure 3a). Note that the fluorine atoms are sequentially attached to both sides of the sheet.

On the basis of these C_2F models, three fluorinated graphene fragments were constructed for the quantum-chemical simulation of the NEXAFS CK edge spectra. The initial graphene fragment was composed from 96 carbon atoms arranged in correspondence with the C_{2h} symmetry. This fragment size was shown to allow obtaining a good agreement between the theoretical X-ray fluorescent spectrum and the experimental spectrum of graphite fluoride $(CF)_n$.[62] The dangling boundary bonds were saturated with fluorine atoms. An additional 16 fluorine atoms were deposited in the central part of the graphene fragment (Figure 3b), forming two parallel zigzag chains (model 1) or armchair chains (model 2) and two strips from the CF−CF bonds (model 3). The CF chains and stripes in the models are separated by corresponding nonfluorinated carbon units. The calculations indicate that the arrangement of fluorine atoms in the zigzag chains is most thermodynamically preferable, while formation of the armchair chains and isolated CF−CF bonds requires additionally 0.11 and 0.28 eV per fluorine atom.

In the considered models, there are two chemically non-equivalent carbon atoms, namely, the carbon atom bonded with a fluorine atom and the bare carbon atom. Hence, two $C_{95}F_{42}N^+$ structures, where a nitrogen atom was substituted for a central carbon atom in the fluorinated unit and in the nonfluorinated unit, were calculated for each model to plot the CK edge spectrum. The resultant spectrum was generated by summing the spectra of the ionized structures with equal weightings. To compare the simulated spectra with experimental data, we took the spectrum recorded at the incidence angle of 45° because this angle provides isotropic behavior of peak intensity at the used geometry of the measurements.[63] The theoretical spectra aligned to the experimental spectrum by the position of the first peak are shown in Figure 3c. The first and second spectral components correspond

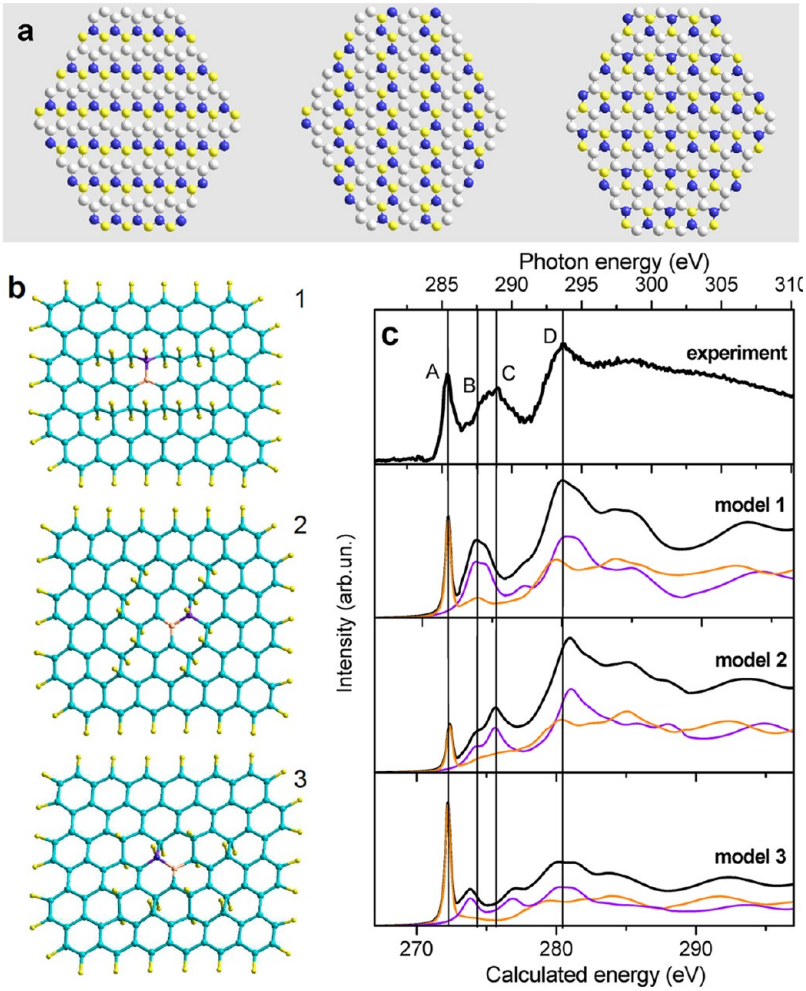

Figure 3. (a) Models of fluorinated graphene with C_2F composition. Left: Alternating zigzag chains of fluorinated carbon and bare carbon. Middle: Alternating armchair chains of fluorinated carbon and bare carbon. Right: Alternating double carbon bonds and CF−CF bonds. White spheres represent the bare carbon atoms; the change in color within the fluorinated unit indicates change of position (up or down) of fluorine atoms relative to the graphene sheet. (b) Fragments of fluorinated graphene with zigzag chain (model 1), armchair chain (model 2), and double bond (model 3) fluorine pattern, calculated at the B3LYP/6-31G level. The central atoms, which were replaced by nitrogen atoms to calculate the $C_{95}F_{42}N^+$ structures, are marked. (c) Comparison of experimental NEXAFS CK edge spectrum of the fluorinated HOPG with theoretical spectra of the models 1, 2, and 3. The components of the theoretical spectrum correspond to a contribution from a bare carbon atom (orange line) and fluorinated carbon atom (violet line).

to the X-ray transitions within, respectively, sp^2-hybridized carbon and carbon bonded with fluorine. The spectra of C_2F models are different in the relative intensity of π^* resonance (peak A) and intensities of the features located between peaks A and D. Among the considered fluorine patterns, formation of isolated C═C bonds in a fluorographene matrix (model 3) is most unlikely because, in this case, the π^* states are strongly localized, giving high relative intensity of peak A. Moreover, the spectrum of model 3 shows a low intensity in the region corresponding to C−F bonds. Intensity of the π^* resonance relative to the σ edge (peak D) observed in the model 1 spectrum gives the best fit to the experiment. However, the intensity of peak C in this theoretical spectrum is underestimated. On the basis of CK edge spectrum modeling, we suggest that room-temperature fluorination of graphite results in preferable formation of zigzag CF chains with probable admixture of armchair CF chains. We emphasize that the suggested C_2F structure is rather crude and additional models should be considered to reveal actual fluorine pattern. Particularly, the present spectra, plotted for the central atoms, correspond to long CF chains and do not account for the contribution from the terminal atoms. The different mutual direction of neighboring C−F bonds can also affect the relative position and intensity of the NEXAFS peaks (Supporting Information, Figure S4). Moreover, in the considered models, the fluorinated graphene regions and nonfluorinated graphene regions have a width of one atom, while in fact, it could vary. For example, our predominant calculations show that a structure, where the zigzag-like fluorinated chains are separated by a hexagonal ribbon

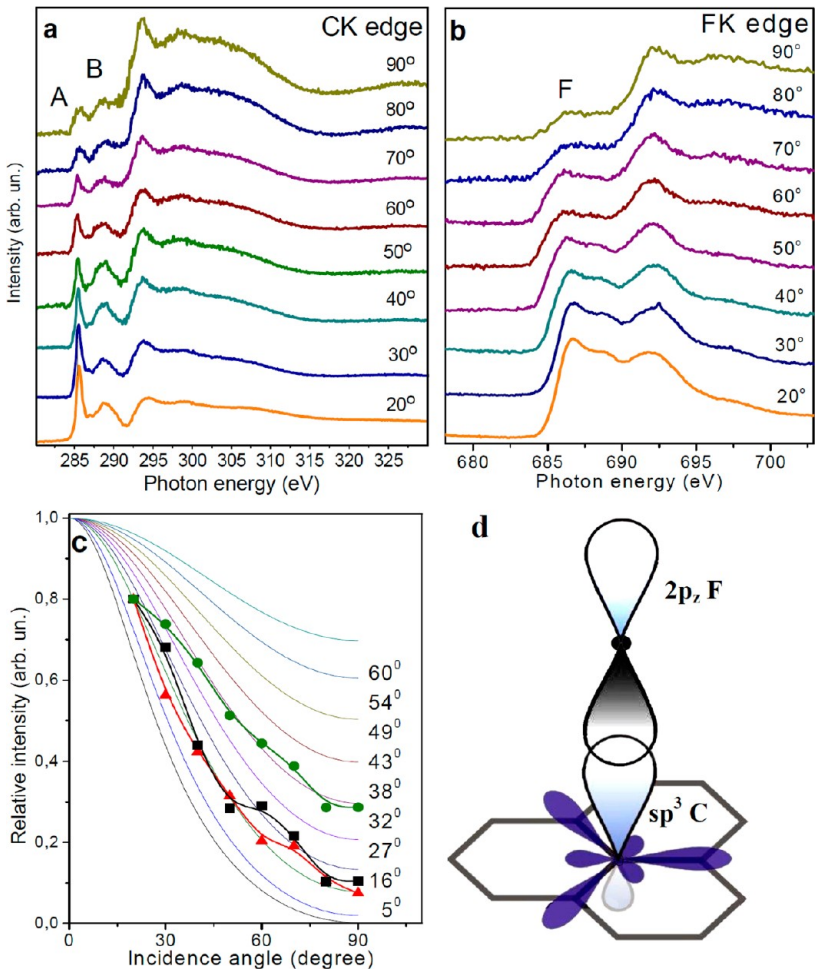

Figure 4. NEXAFS spectra measured near CK edge (a) and FK edge (b) of fluorinated HOPG at different incidence angle of radiation. (c) Angular dependence of the relative intensity of the π^* resonance calculated for different Gaussian distributions of graphene layer orientation (thin lines) in a material compared with the experimental data (triangles and rings correspond to peaks A and B in the CK edge spectrum, and squares correspond to peak F in the FK edge spectrum). (d) Schematic representation of the interaction of a fluorine atom with a carbon atom of the graphene sheet.

(Supporting Information, Figure S5), is only ~0.15 eV less stable than model 1.

Evaluation of Disordering in HOPG with Fluorination. The procedure of vapor fluorination of graphite could cause misorientaion of crystallites, which, as shown by the NEXAFS measurements (Figure 2b), is close to zero in the pristine HOPG. To check the fluorinated sample distortion, we measured the angle-resolved CK and FK edge spectra with a step of 10° (Figure 4a,b). The two main peaks (labeled A and B in Figure 4a) appearing before the CK edge and the first peak (labeled F in Figure 4b) before the FK edge were taken for the analysis. These peaks are well-resolved in the spectra, which allows us to determine their intensity accurately. The angular dependencies of the peak intensity normalized on the spectral intensity at 330 eV in the carbon region and at 750 eV in the fluorine region are shown in Figure 4c. The experimental data are superposed onto the theoretical curves corresponding to the behavior of the relative intensity of π^* resonance on the incidence angle θ of radiation for graphite with a different width of angular orientation of crystallites.[64] The calculation details are presented in the Supporting Information. For ideal graphite, where the basal planes of all crystallites are parallel, the angular orientation width is equal to zero and the π^* resonance intensity follows the $\cos^2\theta$ (the bottom curve in Figure 4c). Experimentally, this dependence has been previously observed for the HOPG, used here for the fluorination.[65] In the case of our semifluorinated graphite, the dependence of peak A originating from the π^* electrons corresponds to an angle of 18°, and this value characterizes the average tilt angle of the carbon network with respect to the holder surface. AFM analysis of a fluorinated flake surface (Figure 1c) indicates that rippling of the graphene network as a result of fluorine bonding corresponds to the disordering of ~5−10°. Additional contribution can be related to a disorientation of layers, caused by penetration of Br_2 and BrF_3 gases through the crystallite boundaries. The resultant cracks are very visible in the optical images of the fluorinated sample surface (Figure 1b).

Thus, we reveal that gas-phase fluorination of HOPG introduces disorder on the microscopic level (graphene rippling) as well as on the macroscopic level (crystallite disorientation).

The similarity between the angular behaviors of peak F of the FK edge spectrum and peak A of the CK edge spectrum is due to the nearly perpendicular orientation of the $2p_z$ orbitals of fluorine atoms to the graphene sheet (Figure 4d). This orientation is possible only in the case of subsequent attachment of fluorine atoms to both sides of graphene. From energy alignment of the CK edge and FK edge spectra (Figure 2), peak B in the CK edge spectrum was assigned to the C−F bonds. However, the angular dependence of the intensity of peak B shows the width distribution of ~32° that is significantly larger than that obtained for peak F. This fact shows the sp^3-hybridized state of carbon atoms bonded with fluorine atoms and, hence, the covalent C−F interactions in the synthesized semifluorinated graphite.

CONCLUSIONS

The room-temperature fluorination of highly ordered graphite using a gaseous mixture of BrF_3 and Br_2 allows producing an optically transparent layered material with a composition close to C_2F. XPS spectroscopy detects two main chemical states of carbon, namely, the carbon atoms bonded with single fluorine atoms and the bare carbon atoms linked with CF groups. Analysis of the angle-resolved NEXAFS data obviously indicates the covalent bonding between carbon and fluorine. In contrast to the high-temperature-produced semifluorinated graphite, in our material, the fluorine atoms are attached on both sides of the graphene sheet and the nonfluorinated carbon atoms preserve their π electrons intact. On the basis of the X-ray spectroscopy data, three models of the fluorinated graphene were considered. The chains (armchair or zigzag) constituted from bare carbon atoms alternated with chains from fluorinated carbon atoms and the double C═C bonds alternated with CF−CF bonds. The theoretical NEXAFS spectra for the models were calculated at the B3LYP/6-31G level within the $Z+1$ approach accounting for the hole−electron interactions. Comparison between the theory and experiment shows that fluorine forms the most likely zigzag chains with an admixture of armchair chains. This finding is supported by the high-resolution AFM image of the fluorinated layer surface. Direction of the chains is determined by the hexagonal graphene lattice, while the chain length is kinetically controlled. The fluorine pattern and hence the size and shape of the π electron regions could be varied by changing the synthesis conditions (duration, temperature, concentration of BrF_3 in Br_2) as well as choosing an appropriate initial graphite sample.

METHODS

Synthesis. The HOPG sample was obtained from the Institute "NII Grafit", Moscow, Russian Federation. A 5 × 5 × 0.1 mm^3 plate was placed in a Teflon flask and held in the vapor over liquid Br_2 for 2 days. The obtained sample, being a second-stage intercalation compound C_8Br, was transferred to another Teflon flask and located over a 10 vol % solution of BrF_3 in Br_2. The use of Br_2 for preliminary graphite intercalation as well as for dilution of the fluorinating agent BrF_3 results in a decrease of the amount of energy released with the fluorination, making the synthetic process safer. Fluorination by gaseous BrF_3 was carried out during 1 month. Thereafter, the flask content was dried by a flow of N_2 until no more Br_2 was released (~48 h).

Characterization and Spectroscopic Studies. Optical images of the fluorinated sample pieces were obtained on an Olympus BX51 TRF microscope. Surface topography was examined using a Solver-Pro NT MDT atomic force microscope (AFM). X-ray photoelectron spectra (XPS) were measured with the excitation energy of 1486 eV on a SPECS spectrometer. The NEXAFS experiments were carried out at the Berliner Elektronenspeicherring für Synchrotronstrahlung (BESSY) using radiation from the Russian−German beamline. The HOPG or fluorinated HOPG plate was split using a knife, and a flake with a thickness of a few micrometers was taken from the inner part of the sample. The flake was fixed to a molybdenum holder in a manner that the sample cleavage plane was parallel to the holder surface. By rotating the holder along the vertical axis, the angle θ of incidence of the X-ray beam polarized in the horizontal plane was varied from 15 to 90°. At the normal angle θ, the irradiated area was ~0.5 mm. The NEXAFS spectra at the K edge of carbon and fluorine atoms were acquired in the total-electron yield mode. In this mode, the secondary electrons escape from a depth of ~10 nm for conductive graphitic materials and ~20−100 nm for insulators such as graphite fluorides, probing the bulk of the samples. The collected spectra were normalized to the primary photon current from a gold-covered grid recorded simultaneously. The monochromatization of the incident radiation was ~80 meV in the carbon absorption region and ~170 meV in the fluorine absorption region, both full width at half-maximum (fwhm). The base pressure in the chamber was ~10^{-9} mbar.

Quantum-Chemical Calculations. The models of fluorinated graphene fragments were calculated using a three-parametric hybrid Becke functional[66] and Lee−Yang−Parr correlation functional[67] (B3LYP method) included in a quantum-chemical package Jaguar.[68] The atomic orbitals were described by a 6-31G basis set. Geometry of the models was optimized by an analytical method to the gradient value of 5 × 10^{-4} atomic units. X-ray transition energies were determined as a difference of the Kohn−Sham one-electron energy of virtual molecular orbitals of a model calculated within the $Z+1$ approximation and the energy of C 1s level taken from the ground-state calculation of this model. Intensities of a spectral line were calculated as a sum of the squared coefficients at N 2p atomic orbitals in the relaxed models and broadened by a Lorentzian function with a fwhm width increasing with energy of an emitting photon.[41]

Conflict of Interest: The authors declare no competing financial interest.

Acknowledgment. We thank Dr. P. N. Gevko for the AFM measurements. The work was partially supported by the bilateral Program "Russian−German Laboratory" at BESSY.

Supporting Information Available: X-ray diffraction pattern, Raman spectrum, X-ray photoelectron F 1s and Br 3d spectra of the fluorinated HOPG, theoretical CK edge spectra simulated for two C_2F models with isolated double bonds and different

mutual orientation of four fluorine atoms in a hexagon, details of calculations of dependences of NEXAFS spectral intensity on the incidence angle of radiation. This material is available free of charge *via* the Internet at http://pubs.acs.org.

REFERENCES AND NOTES

1. Novoselov, K. S.; Geim, A. K.; Morozov, S. V.; Jiang, D.; Zhang, Y.; Dubonos, S. V.; Grigorieva, I. V.; Firsov, A. A. Electric Field Effect in Atomically Thin Carbon Films. *Science* **2004**, *306*, 666–669.
2. Mas-Ballesté, R.; Gómez-Navarro, C.; Gómez-Herrero, J.; Zamore, F. 2D Materials: To Graphene and Beyond. *Nanoscale* **2011**, *3*, 20–30.
3. Dreyer, D. R.; Park, S.; Bielawski, C. W.; Ruoff, R. S. The Chemistry of Graphene Oxide. *Chem. Soc. Rev.* **2010**, *39*, 228–240.
4. Elias, D. C.; Nair, R. R.; Mohiuddin, T. M. G.; Morozov, S. V.; Blake, P.; Halsall, M. P.; Ferrari, A. C.; Boukhvalov, D. W.; Katsnelson, M. I.; Geim, A. K.; *et al.* Control of Graphene's Properties by Reversible Hydrogenation: Evidence for Graphane. *Science* **2009**, *323*, 610–613.
5. Savchenko, A. Transforming Graphene. *Science* **2009**, *323*, 589–590.
6. Nair, R. R.; Ren, W.; Jalil, R.; Riaz, I.; Kravets, V. G.; Britnell, L.; Blake, P.; Schedin, F.; Mayorov, A. S.; Yuan, S.; *et al.* Fluorographene: A Two-Dimensional Counterpart of Teflon. *Small* **2010**, *6*, 2877–2884.
7. Robinson, J. T.; Burgess, J. S.; Junkermeier, C. E.; Badescu, S. C.; Reinecke, T. L.; Perkins, F. K.; Zalalutdniov, M. K.; Baldwin, J. W.; Culbertson, J. C.; Sheehan, P. E.; *et al.* Properties of Fluorinated Graphene Films. *Nano Lett.* **2010**, *10*, 3001–3005.
8. Novoselov, K. S. Nobel Lecture: Graphene: Materials in the Flatland. *Rev. Mod. Phys.* **2011**, *83*, 837–849.
9. Haberer, D.; Vyalikh, D. V.; Taioli, S.; Dora, B.; Farjam, M.; Fink, J.; Marchenko, D.; Pichler, T.; Ziegler, K.; Simonucci, S.; *et al.* Tunable Band Gap in Hydrogenated Quasi-Free-Standing Graphene. *Nano Lett.* **2010**, *10*, 3360–3366.
10. Jeon, K.-J.; Lee, Z.; Pollak, E.; Moreschini, L.; Bostwick, A.; Park, C.-M.; Mendelsberg, R.; Radmilovic, V.; Kostecki, R.; Richardson, T. J.; *et al.* Fluorographene: A Wide Bandgap Semiconductor with Ultraviolet Luminescence. *ACS Nano* **2011**, *5*, 1042–1046.
11. Geim, A. Graphene: Status and Prospects. *Science* **2009**, *324*, 1531–1534.
12. Withers, F.; Dubois, M.; Savchenko, A. K. Electron Properties of Fluorinated Single-Layer Graphene Transistors. *Phys. Rev. B* **2010**, *82*, 073403.
13. Cheng, S.-H.; Zou, K.; Okino, F.; Gutierrez, H. R.; Gupta, A.; Shen, N.; Eklund, N.; Sofo, J. O.; Zhu, J. Reversible Fluorination of Graphene: Evidence of a Two-Dimensional Wide Bandgap Semiconductor. *Phys. Rev. B* **2010**, *81*, 205435.
14. Watanabe, N.; Nakajima, T.; Touhara., H. *Studies in Inorganic Chemistry 8. Graphite Fluorides*; Elsevier: Amsterdam, 1988.
15. Kamarchik, P., Jr.; Margrave, J. L. Poly(carbon monofluoride), a Solid Layered Fluorocarbon. *Acc. Chem. Res.* **1978**, *11*, 296–300.
16. Charlier, J.-C.; Gonze, X.; Michenaud, J.-P. First-Principles Study of Graphite Monofluoride $(CF)_n$. *Phys. Rev. B* **1993**, *47*, 16162.
17. Leenaerts, O.; Peelaers, H.; Hernández-Nieves, A. D.; Partoens, B.; Peeters, F. M. First-Principles Investigation of Graphene Fluoride and Graphane. *Phys. Rev. B* **2010**, *82*, 195436.
18. Samarakoon, D. K.; Chen, Z.; Nicolas, C.; Wang, X.-Q. Structural and Electronic Properties of Fluorographene. *Small* **2011**, *7*, 965–969.
19. Kita, Y.; Watanabe, N.; Fujii, Y. Chemical Composition and Crystal Structure of Graphite Fluoride. *J. Am. Chem. Soc.* **1979**, *101*, 3832–3841.
20. Touhara, H.; Okino, F. Property Control of Carbon Materials by Fluorination. *Carbon* **2000**, *38*, 241–267.
21. Sato, Y.; Itoh, K.; Hagiwara, R.; Fukunaga, T.; Ito, Y. Short-Range Structures of Poly(dicarbon monofluoride) $(C_2F)_n$ and Poly(carbon monofluoride) $(CF)_n$. *Carbon* **2004**, *42*, 2897–2903.
22. Mallouk, T.; Bartlett, N. Reversible Intercalation of Graphite by Fluorine: A New Bifluoride, $C_{12}HF_2$, and Graphite Fluorides, C_xF ($5 > x > 2$). *J. Chem. Soc., Chem. Commun.* **1983**, 103–105.
23. Makotchenko, V. G.; Nazarov, A. S.; Yakovlev, I. I. Intercalation of Poly(tetracarbon monofluoride) with Iodine Pentafluoride. *Inorg. Mater.* **1999**, *35*, 1186–1187.
24. Yudanov, N. F.; Chernyavskii, L. I. Model for the Structures of Intercalation Compounds Based on Graphite Fluoride. *J. Struct. Chem.* **1987**, *28*, 534–541.
25. Mitkin, V. N. Types of Inorganic Fluorocarbon Polymer Materials and Structure—Property Correlation Problems. *J. Struct. Chem.* **2003**, *44*, 82–115.
26. Bulusheva, L. G.; Okotrub, A. V.; Yudanov, N. F. Atomic Arrangement and Electronic Structure of Graphite Fluoride C_2F. *Phys. Chem. Mater. Low-Dimens. Struct.* **2002**, *7/8*, 1–14.
27. Makarova, T. L.; Zagaynova, V. S.; Inan, G.; Okotrub, A. V.; Chekhova, G. N.; Pinakov, D. V.; Bulusheva, L. G. Structural Evolution and Magnetic Properties of Underfluorinated C_2F. *J. Supercond. Novel Magn.* **2012**, *25*, 79–83.
28. Bulusheva, L. G.; Kasyanov, S. L.; Okotrub, A. V. Electronic Structure of Graphite Fluorides: Band Model and Cluster Calculations. *Phys. Chem. Mater. Low-Dimens. Struct.* **1998**, *11/12*, 189–202.
29. Han, S. S.; Yu, T. H.; Merinov, B. V.; Van Duin, A. C. T.; Yazami, R.; Goddard, W. A., III. Unraveling Structural Models of Graphite Fluorides by Density Functional Theory Calculations. *Chem. Mater.* **2010**, *22*, 2142–2154.
30. Hemraj-Benny, T.; Banerjee, S.; Sambasivan, S.; Balasubramanian, M.; Fisher, D. A.; Eres, G.; Puretzky, A. A.; Geohegan, D. B.; Lowndes, D. H.; Han, W.; *et al.* Near-Edge X-ray Absorption Fine Structure Spectroscopy As a Tool for Investigating Nanomaterials. *Small* **2006**, *1*, 26–35.
31. Seki, K.; Mitsumoto, R.; Itoc, E.; Araki, T.; Sakurai, Y.; Yoshimura, D.; Ishii, H.; Ouchi, Y.; Miyamae, T.; Narita, T.; *et al.* High-Energy Spectroscopic Studies of the Electronic Structures of Organic Systems Formed from Carbon and Fluorine by UPS, Vacuum-UV Optical Spectroscopy, and NEXAFS: Poly(hexafluoro-1,3-butadiene) $[C(CF_3) = C(CF_3)]_n$, Fluorinated Graphites (CF, C_2F, and C_6F), Perfluoroalkanes n-C_nF_{2n+2}, Poly(tetrafluoroethylene) $(CF_2)_n$, and Fluorinated Fullerenes ($C_{60}F_x$ and $C_{70}F_x$). *Mol. Cryst. Liq. Cryst.* **2001**, *355*, 247–274.
32. Brühwiler, P. A. Synchrotron Studies of Carbon Surfaces. *J. Phys.: Condens. Mater.* **2001**, *13*, 11229–11248.
33. Muramatsu, Y.; Kaneyoshi, T.; Gullokson, E. M.; Perera, R. C. C. Angle-Resolved Soft X-ray Emission and Absorption Spectroscopy of Hexagonal Boron Nitride. *Spectrochim. Acta, Part A* **2003**, *59*, 1951–1957.
34. Li, Z.; Zhang, L.; Resasco, D. E.; Mun, B. S.; Requejo, F. G. X-ray Absorption Near Edge Structure Study of Vertically Aligned Single-Walled Carbon Nanotubes. *Appl. Phys. Lett.* **2007**, *90*, 103115–103117.
35. Papagno, M.; Fraile Rodríguez, A.; Girit, C. Ö.; Meyer, J. C.; Zettl, A.; Pacilé, D. Polarization-Dependent C K Near-Edge X-ray Absorption Fine-Structure of Graphene. *Chem. Phys. Lett.* **2009**, *475*, 269–271.
36. Pacilé, D.; Meyer, J. M.; Fraile Rodríguez, A.; Papagno, M.; Gómez-Navarro, C.; Sundaram, R. S.; Burghard, M.; Kern, K.; Carbone, C.; Kaiser, U. Electronic Properties and Atomic Structure of Graphene Oxide Membranes. *Carbon* **2011**, *49*, 966–972.
37. Lee, V.; Whittaker, L.; Jaye, L.; Baroudi, K. M.; Fischer, D. A.; Banerjee, S. Large-Area Chemically Modified Graphene Films: Electrophoretic Deposition and Characterization by Soft X-ray Absorption Spectroscopy. *Chem. Mater.* **2009**, *21*, 3905–3916.
38. Brühwiler, P. A.; Maxwell, A. J.; Puglia, C.; Nilsson, A.; Andersson, S.; Mårtensson, N. π- and σ-Exitons in C-1s Absorption of Graphite. *Phys. Rev. Lett.* **1995**, *74*, 614.

39. Schwarz, W. H. E. Interpretation of the Core Electron Excitation Spectra of Hydride Molecules and the Properties of Hydride Radicals. *Chem. Phys.* **1975**, *11*, 217–228.
40. Nyberg, M.; Luo, Y.; Triquero, L.; Pettersson, L. G. M.; Ågren, H. Core-Hole Effects in X-ray-Absorption Spectra of Fullerenes. *Phys. Rev. B* **1999**, *60*, 7956.
41. Bulusheva, L. G.; Okotrub, A. V.; Shnitov, V. V.; Bryzgalov, V. V.; Boltalina, O. V.; Gol'dt, I. V.; Vyalikh, D. V. Electronic Structure of $C_{60}F_{36}$ Studied by Quantum-Chemical Modeling of Experimental Photoemission and X-ray Absorption Spectra. *J. Chem. Phys.* **2009**, *130*, 014704.
42. Fedosseva, Yu. V.; Bulusheva, L. G.; Okotrub, A. V.; Asanov, I. P.; Troyanov, S. I.; Vyalikh, D. V. Electronic Structure of the Chlorinated Fullerene $C_{60}Cl_{30}$ Studied by Quantum Chemical Modeling of X-ray Absorption Spectra. *Int. J. Quantum Chem.* **2011**, *111*, 2688–2695.
43. Hua, W.; Gao, B.; Li, S.; Ågren, H.; Luo, Y. X-ray Absorption Spectra of Graphene from First-Principles Simulations. *Phys. Rev. B* **2010**, *82*, 155433.
44. Bulusheva, L. G.; Okotrub, A. V.; Lavskaya, Yu. V.; Vyalikh, D. V.; Dettlaff-Weglikowska, U.; Fonseca, A.; Hata, K. Comparative NEXAFS Examination of Single-Wall Carbon Nanotubes Produced by Different Methods. *Phys. Status Solidi B* **2009**, *11*−*12*, 2637–2640.
45. Yang, D.-Q.; Sacher, E. Carbon 1s X-ray Photoemission Line Shape Analysis of Highly Oriented Pyrolytic Graphite: The Influence of Structural Damage on Peak Asymmetry. *Langmuir* **2006**, *22*, 860–862.
46. Okotrub, A. V.; Asanov, I. P.; Yudanov, N. F.; Babin, K. S.; Gusel'nikov, A. V.; Nedoseikina, T. I.; Gevko, P. N.; Bulusheva, L. G.; Osváth, Z.; Biró, L. P. Development of Graphene Layers by Reduction of Graphite Fluoride C_2F Surface. *Phys. Status Solidi B* **2009**, *246*, 2545–2548.
47. Plank, N. O. V.; Jiang, L.; Cheung, R. Fluorination of Carbon Nanotubes in CF_4 plasma. *Appl. Phys. Lett.* **2003**, *83*, 2426–2428.
48. Asanov, I. P.; Paasonen, V. M.; Mazalov, L. N.; Nazarov, A. S. X-ray Photoelectron Study of Fluorinated Graphite Intercalation Compounds. *J. Struct. Chem.* **1998**, *39*, 928–932.
49. Papirer, E.; Lacroix, R.; Donnet, J.-B.; Nanse, G.; Fioux, P. XPS Study of the Halogenation of Carbon Black—Part 1. Bromination. *Carbon* **1994**, *32*, 1341–1358.
50. Rosenberg, R. A.; Love, P. J.; Rehn, V. Polarization-Dependent C(K) Near-Edge X-ray-Absorption Fine-Structure of Graphite. *Phys. Rev. B* **1986**, *33*, 4034.
51. Ma, Y.; Skytt, P.; Wassdahl, N.; Glans, P.; Mancini, D. C.; Guo, J.; Nordgren, J. Core Excitons and Vibronic Coupling in Diamond and Graphite. *Phys. Rev. Lett.* **1993**, *71*, 3725.
52. Castrucci, P.; Scarselli, M.; De Crescenzi, M.; El Khakani, M. A.; Rosei, F. Probing the Electronic Structure of Carbon Nanotubes by Nanoscale Spectroscopy. *Nanoscale* **2010**, *2*, 1611–1625.
53. Watts, B.; Ade, H. A Simple Method for Determining Linear Polarization and Energy Calibration of Focused Soft X-ray Beams. *J. Electron Spectrosc. Relat. Phenom.* **2008**, *162*, 49.
54. Fischer, D. A.; Wentzcovitch, R. M.; Carr, R. G.; Continenza, A.; Freeman, A. J. Graphitic Interlayer States—A Carbon-K Near-Edge X-ray Absorption Fine-Structure Study. *Phys. Rev. B* **1991**, *44*, 1427.
55. Pacilé, D.; Papagno, M.; Fraile Rodríguez, A.; Grioni, M.; Papagno, L. Near-Edge X-ray Absorption Fine-Structure Investigation of Graphene. *Phys. Rev. Lett.* **2008**, *101*, 066806.
56. Jeong, H.-K.; Noh, H.-J.; Kim, J.-Y.; Colakerol, L.; Glans, P.-A.; Jin, M. H.; Smith, K. E.; Lee, Y. H. Comment on "Near-Edge X-ray Absorption Fine-Structure Investigation of Graphene". *Phys. Rev. Lett.* **2009**, *102*, 099701.
57. Kiguchi, M.; Takai, K.; Joseph Joly, V. L.; Enoki, T.; Sumii, R.; Amemiya, K. Observation of Magnetic Edge State and Dangling Bond State on Nanographene in Activated Carbon Fibers. *Phys. Rev. B* **2011**, *84*, 045421.
58. Lavskaya, Yu. V.; Bulusheva, L. G.; Okotrub, A. V.; Yudanov, N. F.; Vyalikh, D. V.; Fonseca, A. Comparative Study of Fluorinated Single- and Few-Wall Carbon Nanotubes by X-ray Photoelectron and X-ray Absorption Spectroscopy. *Carbon* **2009**, *47*, 1629–1636.
59. Bulusheva, L. G.; Fedoseeva, Yu. V.; Okotrub, A. V.; Flahaut, E.; Asanov, I. P.; Koroteev, V. O.; Yaya, A.; Ewels, C. P.; Chuvilin, A. L.; Felten, A.; *et al.* Stability of Fluorinated Double-Walled Carbon Nanotubes Produced by Different Fluorination Techniques. *Chem. Mater.* **2010**, *22*, 4197–4203.
60. Şahin, H.; Topsakal, M.; Ciraci, S. Structures of Fluorinated Graphene and Their Signatures. *Phys. Rev. B* **2011**, *83*, 115432.
61. Osuna, S.; Torrent-Sucarrat, M.; Solà, M.; Geerlings, P.; Ewels, C. P.; Van Lier, G. Reaction Mechanisms for Graphene and Carbon Nanotube Fluorination. *J. Phys. Chem. C* **2010**, *114*, 3340–3345.
62. Bulusheva, L. G.; Okotrub, A. V. Nature of Chemical Bonding in the Fluorinated Carbon Compounds. *Rev. Inorg. Chem.* **1999**, *19*, 79–115.
63. Belavin, V. V.; Okotrub, A. V.; Bulusheva, L. G.; Kotosonov, A. S.; Vyalykh, D. V.; Molodtsov, S. L. Determining Misorientation of Graphite Grains from the Angular Dependence of X-ray Emission Spectra. *J. Exp. Theor. Phys.* **2006**, *103*, 604–610.
64. Okotrub, A. V.; Belavin, V. V.; Bulusheva, L. G.; Gusel'nikov, A. V.; Kudashov, A. G.; Vyalykh, D. V.; Molodtsov, S. L. Determination of the Texture of Arrays of Aligned Carbon Nanotubes from the Angular Dependence of the X-ray Emission and X-ray Absorption Spectra. *J. Exp. Theor. Phys.* **2008**, *107*, 517–525.
65. Okotrub, A. V.; Kanygin, M. A.; Sedelnikova, O. V.; Gusel'nikov, A. V.; Kotosonov, A. S.; Bulusheva, L. G. Interaction of Ultrasoft X-rays with Arrays of Aligned Carbon Nanotubes. *J. Nanophotonics* **2010**, *4*, 041655.
66. Becke, A. D. A. Density-Functional Thermochemistry III. The Role of Exact Exchange. *J. Chem. Phys.* **1993**, *98*, 5648–5652.
67. Lee, C.; Yang, W.; Parr, R. G. Development of the Colle-Solvetti Correlation-Energy Formula into a Functional of the Electron Density. *Phys. Rev. B* **1988**, *37*, 785–789.
68. *Jaguar*, version 7.8; Schrödinger, LLC: New York, NY, 2011.